Title

B Cells Regulate Macrophage Phenotype and Response to Chemotherapy in Squamous Carcinomas

Journal

Cancer Cell, 25(6)

ISSN

1535-6108

Authors

Affara, Nesrine I
Ruffell, Brian
Medler, Terry R
et al.

Publication Date

2014-06-01

DOI

10.1016/j.ccr.2014.04.026

Peer reviewed

Published in final edited form as:
Cancer Cell. 2014 June 16; 25(6): 809–821. doi:10.1016/j.ccr.2014.04.026.

B cells Regulate Macrophage Phenotype and Response to Chemotherapy in Squamous Carcinomas

Nesrine I. Affara[#1], **Brian Ruffell**[#1,5,8], **Terry R. Medler**[5], **Andrew J. Gunderson**[5], **Magnus Johansson**[1], **Sophia Bornstein**[7], **Emily Bergsland**[2,4], **Martin Steinhoff**[3], **Yijin Li**[9], **Qian Gong**[9], **Yan Ma**[9], **Jane F. Wiesen**[1,5], **Melissa H. Wong**[5,6,8], **Molly Kulesz-Martin**[5,6,8], **Bryan Irving**[9,10], and **Lisa M. Coussens**[1,4,5,8,*]

[1]Department of Pathology, University of California, San Francisco, CA 94143, USA

[2]Department of Medicine, University of California, San Francisco, CA 94143, USA

[3]Department of Dermatology, University of California, San Francisco, CA 94143, USA

[4]Helen Diller Family Comprehensive Cancer Center, University of California, San Francisco, CA 94143, USA

[5]Department of Cell and Developmental Biology, Oregon Health and Science University, Portland, OR 97239, USA

[6]Department of Dermatology Oregon Health and Science University, Portland, OR 97239, USA

[7]Department of Radiation Medicine, Oregon Health and Science University, Portland, OR 97239, USA

[8]Knight Cancer Institute, Oregon Health and Science University, Portland, OR 97239, USA

[9]Genentech, South San Francisco, CA 94080, USA

[#] These authors contributed equally to this work.

SUMMARY

B cells foster squamous cell carcinogenesis (SCC) through deposition of immunoglobulin-containing immune complexes in premalignant tissue and Fcγreceptor-dependent activation of myeloid cells. Since human SCCs of the vulva and head and neck exhibited hallmarks of B cell infiltration, we examined B cell-deficient mice and found reduced ability to support SCC growth. Although ineffective as a single agent, treatment of mice bearing pre-existing SCCs with B cell-depleting αCD20 monoclonal antibodies improved response to platinum- and taxol-based chemotherapy. Improved chemo-responsiveness was dependent on altered chemokine expression by macrophages that fostered tumor infiltration of activated $CD8^+$ T cells via CCR5-dependent

[*]**Address for correspondence:** L.M. Coussens, Ph.D. Cell & Developmental Biology Oregon Health & Sciences University 3181 SW Sam Jackson Park Rd, Mail Code L215, Rm 5508, Richard Jones Hall Portland, OR 97239-3098 **coussenl@ohsu.edu**.
[10]Current Address: CytomX Therapeutics, South San Francisco, CA 94080, USA

mechanisms. These data reveal that B cells, and the downstream myeloid-based pathways they regulate, represent tractable targets for anti-cancer therapy in select tumors.

Keywords

Cancer; B cell; CD8 T cell; macrophage; humoral immunity; immunoglobulin; inflammation; CD20; chemotherapy

INTRODUCTION

As the central component of humoral immunity, B lymphocytes function in immunoglobulin (Ig) production, antigen presentation and secretion of pro-inflammatory cytokines. While critical for combating pathogens and aiding tissue healing, population-based studies have revealed increased systemic humoral immune responses, including increased deposition of Ig into tissues, in individuals afflicted with some chronic inflammatory disorders associated with increased cancer risk. Cancer patients often develop antibodies to tumor-associated antigens; however, production of these does not necessarily confer protection, but instead often correlates with poor prognosis and decreased survival for several human cancer types. Population-based and experimental studies indicate that anti-tumor antibodies can facilitate tumor growth by promoting protumor immune responses and in general protecting malignant cells from cytotoxic T cell (CTL)-mediated killing (Gunderson and Coussens, 2013; Tan and Coussens, 2007), thus supporting a role for B cells and humoral immunity in fostering cancer development. Support for a protumor role for B cells is further provided by the realization that growth of some subcutaneous solid tumors is retarded in syngeneic B cell-deficient mice, associated with enhanced local expression of T helper (T_H)1 cytokines and increased infiltration of tumors by CTLs (Qin et al., 1998; Shah et al., 2005; Tadmor et al., 2011).

Using a transgenic mouse model of de novo squamous cell carcinoma (SCC) development (Coussens et al., 1996), we reported that B cells and humoral immunity foster SCC development by activating Fcγ receptors (FcγRs) on resident and recruited myeloid cells (Andreu et al., 2010; de Visser et al., 2005). Rather than infiltrating premalignant skin, immunoglobulin (Ig)-secreting B cells exert distal effects on neoplastic tissue via production of circulating immune complexes (CIC) that accumulate in premalignant tissue (Andreu et al., 2010; de Visser et al., 2005). Following CIC engagement of activating-type I and III FcγRs, tumor progression is fostered through activation of proangiogenic, tissue remodeling and pro-survival pathways in resident and recruited myeloid cells, in particular macrophages and mast cells (Andreu et al., 2010). Based on these data, we hypothesized that B cells, and the downstream myeloid-based pathways they regulate, represented tractable targets for combinatorial therapy in SCC. We therefore examined the preclinical efficacy of a B cell-depleting αCD20 mAb as an anti-cancer monotherapy, and in combination with chemotherapy (CTX).

RESULTS

B cells in human solid tumors

Unlike squamous carcinoma development in mice wherein premalignant and malignant tissues are poorly infiltrated by B cells (Andreu et al., 2010; de Visser et al., 2005; Schioppa et al., 2011), formation of tertiary/ectopic lymphoid structures containing B cells has been described for several human malignancies, including breast, cervical, ovarian, and non-small cell lung cancer (Kobayashi et al., 2002; Nelson, 2010). Based upon these data, we hypothesized that ectopic production of either Ig or CD20 mRNA might signify human cancers wherein the humoral immune response fosters neoplastic progression or tumor growth, and thus identify carcinomas potentially amenable to B cell-targeted therapies.

To address this, we queried cDNA microarray data on a panel of human tumors from the BioExpress® System and assessed CD20 (*MS4A1*) and Ig (*IGHG1*, *IGHG2*, *IGHV4-31*, *IGHM*) mRNA expression relative to corresponding normal tissue. Multiple tumor types displayed increased CD20 or Ig expression as compared to nonmalignant tissue counterparts, but vulva SCCs and head and neck squamous cell carcinomas (HNSCC) exhibited the greatest increase in CD20 and Ig mRNA expression, respectively (**Fig. 1A-B, S1A**), consistent with increased presence of $CD20^+$ B cells in skin, vulva, and head and neck SCC as revealed by immunodetection (**Fig 1C-D**). Several Ig and FcR mRNAs were also found to be differentially expressed in HNSCC tumors relative to normal mucosa based on evaluation of a previously published dataset (Ginos et al., 2004) using Oncomine (Rhodes et al., 2004) (**Fig. S1B**). Notably, etiology for both vulva and HNSCC are in part linked to human papillomavirus (HPV), with increasing incidence of carcinomas in both reflecting higher rates of HPV infection (Chaturvedi, 2010; Chaturvedi et al., 2011).

We have previously established that progression to carcinoma in a murine model of HPV16-induced SCC development (i.e. K14-HPV16 mice) is dependent on binding of Igs to activating FcγRs on infiltrating myeloid cells (Andreu et al., 2010). Importantly, K14-HPV16 mice are not tolerant to HPV oncoproteins (Andreu et al., 2010; Daniel et al., 2005), reflecting a similar scenario in HPV-positive oropharyngeal cancer wherein HPV-specific peripheral blood $CD8^+$ T cells have been described (Albers et al., 2005; Wansom et al., 2010). We therefore sought to evaluate the therapeutic efficacy of B cell-depletion (i.e. αCD20 mAbs) or inhibition of Fcγ signaling via a selective Syk inhibitor (i.e. fostamatinib/R788) (Braselmann et al., 2006; Colonna et al., 2010), in either slowing or blocking progression of premalignant hyperplasia to dysplasia/carcinoma in situ.

Prevention of premalignant dysplasia by B cell-depletion or Syk kinase inhibition

B cells, including mature B cells and plasma cells, accumulate in lymphoid organs of K14-HPV16 mice when neoplastic skin is at an early premalignant stage (**Fig. S2A-G**). Accordingly, we conducted a prevention trial treating K14-HPV16 mice starting at 1-month (mo) of age, with αCD20 mAbs to effectively deplete B cells, as well as with the potent Syk (spleen tyrosine kinase) inhibitor R788/fostamatinib, starting at 1-month (mo) of age when neoplastic skin exhibited a low-grade hyperplastic state throughout, and continuing to 4-mo of age when neoplastic skin instead contained focal areas of low/high-grade dysplasia (**Fig.**

2A). R788 is an orally bioavailable small molecule with potent Syk kinase inhibitory activity, whose active metabolite (R406) binds the ATP binding pocket of Syk and inhibits its kinase activity as an ATP-competitive inhibitor (K_i =30 nM) (Bahjat et al., 2008; Braselmann et al., 2006). Syk plays a key role in signaling downstream of activating FcRs and B cell receptors (BCR), and in several other cell lineages where activation leads to phosphorylation (pSyk) and signal transduction via activation of PLCγ and/or AKT. Notably, expression of mRNAs for both Syk and Bruton's tyrosine kinase (BTK), another key signaling molecule downstream of FcRs and BCRs, were increased in HNSCC tumors relative to normal mucosa (**Fig. S1B**). Phosphorylated BTK was also prominent in HNSCC tissue sections in $CD20^+$ B cells and other stromal cells, as compared to normal mucosa (**Fig. 1C)**.

Administration of αCD20 mAbs to K14-HPV16 mice effectively depleted B cells in peripheral blood and secondary lymphoid organs (**Fig. S2H-L**), including a partial depletion of $CD19^+CD1d^{hi}CD5^+$ B regulatory cells (**Fig. S2M**), a subset of $CD23^{lo}CD21^{hi}$ marginal zone (MZ) B cells (**Fig. S4b**) implicated in repressing anti-tumor immunity in two-stage skin carcinogenesis (Schioppa et al., 2011), and in suppressing lymphoma (Horikawa et al., 2011). Critically, αCD20 mAb treatment reduced levels of circulating IgG_1 (**Fig. S2N**) and presence of autoantibodies against collagen I (**Fig. S2O**), and consistent with a role of CIC deposition in skin of fostering neoplastic progression via FcγRs, treatment with either αCD20 mAb or fostamatinib effectively blocked progression to dysplasia in the prevention trial (**Fig. 2B**).

Since Ig deposition into neoplastic skin of K14-HPV16 mice becomes pronounced between 2- and 3-mo of age, we also conducted an intervention trial where 3-mo old K14-HPV16 mice with high-grade hyperplasia/low-grade focal dysplasia were treated with αCD20 mAbs to 6-mo of age, when neoplastic skin exhibited broadly dysplastic regions of focal high-grade dysplasia/carcinoma in situ (**Fig. 2A**). In this setting as well, B cell depletion via αCD20 mAb as monotherapy blocked progression to dysplasia, and significantly, induced regression to a hyperplastic phenotype (**Fig. 2B**).

Impaired progression to dysplasia in both trials was associated with significantly reduced infiltration of neoplastic skin by $CD45^+$ leukocytes (**Fig. 2C**), encompassing reduced recruitment of $CD11b^+Gr1^+F4/80^-CD11c^-$ immature myeloid cells (iMC), mast cells and $Gr1^+$ cells, with increased infiltration by $CD11b^+Gr1^-$ $F4/80^+CD11c^-$ macrophages, and T cells (**Fig. 2D, S2P-S**), similar to results reported for K14-HPV16/B cell-deficient and K14-HPV16/FcRγ-deficient mice (Andreu et al., 2010). In addition to limiting mast cell infiltration, R406, the active metabolite of fostamatinib, significantly reduced release of interleukin (IL)-4, tumor necrosis factor (TNF)α, IL-23, IL-9, and transforming growth factor (TGF)β from IgG-stimulated bone marrow-derived mast cells (BMMC) in ex vivo assays (**Fig. S2T)**.

Moreover, similar to results reported for K14-HPV16/B cell-deficient and K14-HPV16/FcRγ-deficient mice (Andreu et al., 2010), the reduced and altered infiltration by leukocytes in αCD20 mAb and fostamatinib-treated K14-HPV16 mice was associated with decreased development of angiogenic vasculature (**Fig. 2E**), that translated into diminished

keratinocyte hyperproliferation (**Fig. 2F**). Taken together, these data indicate that B cell depletion and Syk kinase inhibition may represent therapeutic opportunities for prevention and/or intervention in K14-HPV16-positive squamous neoplasms.

B cell-deficient mice fail to support orthotopic SCC tumor growth

Given the increased expression of Ig mRNA in human SCCs **(Fig. 1)** and efficacy of αCD20 mAb in restricting premalignant progression in K14-HPV16 transgenic mice (**Fig. 2**), we next sought to evaluate the anti-tumor efficacy of B cell-depletion as either monotherapy or in combination with CTX. For this, we utilized SCC cell lines derived from K14-HPV16 mice (Arbeit et al., 1996) harboring de novo grade I well-differentiated (WDSC1) or poorly-differentiated SCCs (PDSC5 clone 6). Similar to our results in syngeneic FcRγ-deficient mice (Andreu et al., 2010), orthotopic SCC growth was significantly reduced in syngeneic B cell deficient ($JH^{-/-}$) mice (**Fig. 3A-B**), characterized by increased presence of $CD45^+$ leukocytes, decreased bromodeoxyuridine (BrdU)-positive keratinocytes, increased cleaved caspase 3-positive cells, and decreased tumor vascularization, along with increased presence of $CD8^+$ T cells (**Fig. S3A)**.

Neoadjuvant αCD20 mAb as monotherapy and in combination with chemotherapy

These findings provided a compelling rationale for assessing αCD20 mAb in a therapeutic setting. Thus, we evaluated αCD20 mAb for efficacy in blocking development of syngeneic SCCs, as compared to slowing or inducing regression of preexistent syngeneic SCCs. Mice were administered αCD20 mAb either at the time of tumor cell implantation and again at 2 week intervals (d0; q14d), or instead when orthotopic tumors reached ~50 mm^3 (d12), and then q14d (**Fig. 3C**). Using this strategy, $CD19^+B220^+CD138^-$ mature B cells were efficiently depleted from lymphoid organs (spleen and bone marrow) (**Fig. S3B**), culminating in reduced presence of circulating IgG_1 (**Fig. S3C)**. Whereas administration of αCD20 mAb concurrent with SCC implantation significantly slowed tumor growth to end-stage (**Fig. 3C, Fig. S3D**), accompanied by reduced development of angiogenic vasculature (**Fig. S3E**), tumor growth was not significantly slowed when αCD20 mAb therapy was initiated after tumors were apparent (**Fig. 3C, Fig. S3D-E**), in spite of a significantly increased percentage of $CD8^+$ T cells infiltrating tumors (**Fig. 3D, Fig. S3E)**.

Based on the increased presence of $CD8^+$ T cells in orthotopic SCCs of αCD20 mAb-treated mice we reasoned that efficacy might be enhanced by combination treatment with CTX. Indeed, treatment of mice bearing pre-existent SCCs with αCD20 mAb in combination with cisplatin (CDPP) resulted in tumor regression in all animals (**Fig. S4A**), as compared to CDPP alone, which was without effect. However, mice treated with αCD20/CDPP exhibited a 50% survival rate, likely due to cumulative impairment of liver and renal function (**Fig. S4B**), a clinically relevant outcome as it mirrors CDPP-associated renal toxicity in cancer patients administered concomitant rituximab (αCD20 mAb). Due to its reduced nephrotoxicity, we instead evaluated carboplatin (CBDCA) as an alternative alkylating-type cytotoxic agent that also had no significant effect on tumor growth alone, but significantly slowed tumor growth when combined with αCD20 mAb throughout duration of the CTX cycle (**Fig. 4A**), without evidence of toxicity or morbidity (**Fig. S4B**), thus achieving a more favorable outcome.

To determine if enhanced response to CTX was restricted to platinum-based agents, we next evaluated the microtubule polymer stabilizer paclitaxel (PTX) in combination with αCD20 mAb, and similarly found significantly slowed SCC growth during the treatment cycle (**Fig. 4B**), associated with decreased serum IgG_1(**Fig. S4C**). Histological evaluation of tumors from combinatorial-treated mice revealed reduced malignant keratinocyte proliferation, that was paralleled by increased cell death (cleaved caspase 3-positivity; **Fig. 4C**), reduced angiogenic programming of tumors ($CD31^+$ vessels; **Fig. 4C, S4D**), with no apparent change in vascular leakage as measured by Evans blue assay (**Fig. S4D**).

Given that αCD20 mAb improved responsiveness to PTX, we assessed the durability of tumor repression after 1 cycle of combined αCD20/PTX therapy, and found that tumor regrowth was apparent within 10 days following cessation of PTX (**Fig. 4D**). Since resistance to cytotoxic agents represents a major limitation of CTX, we evaluated a second cycle of αCD20/PTX therapy and found that tumors again responded to combined therapy, but again, that regrowth was evident following cessation of CTX (**Fig. 4D**).

T cell infiltration in αCD20/PTX-treated tumors

To identify cellular mechanisms underlying slowing of tumor growth and increased efficacy of PTX in αCD20-treated mice, we evaluated leukocyte complexity of orthotopic SCCs by flow cytometry and found that SCCs responding to αCD20/PTX contained significantly increased infiltrates of both $CD4^+$ and $CD8^+$ T cells, as compared to tumors that regained growth kinetics following therapy cessation (**Fig. 4D**). Increased $CD8^+$ T cell infiltration in responding tumors from αCD20/PTX-treated mice was not unique to this experimental setting, as when we analyzed neoplastic skin from 4-mo old K14-HPV16/B cell-deficient, HK14-PV16/FcRγ-deficient, and K14-HPV16 mice enrolled in the intervention trial with αCD20 mAbs (**Fig. 1**), we similarly observed increased presence of $CD8^+$ T cells across all experimental groups as compared to controls (**Fig. 4E**). To reveal the functional significance of increased T cell infiltrates, $CD4^+$ and $CD8^+$ T cells were individually depleted from SCC-bearing αCD20/PTX-treated mice (**Fig. S5A**), thus revealing that improved PTX responses in αCD20 mAb-treated mice were $CD8^+$ T cell-dependent (**Fig. 5A**), but $CD4^+$ T cell-independent (**Fig. S5B**). Moreover, depletion of $CD8^+$ T cells reinstated the characteristic density of $CD31^+$ vessels to growing tumors (**Fig. S5C**).

To reveal molecular mediators regulating productive $CD8^+$ T cell activity, we evaluated cytokine mRNA expression in SCCs of treated mice and found significantly increased levels of interferon-alpha (*IFN*α) and granzyme B (*GzmB*), molecules involved in regulating $CD8^+$ T cell activity (**Fig. 5B**). In addition, this analysis revealed increased expression of the angiostatic molecules angiopoietin-1 *(Ang1)* and *CXCL10*, consistent with reduced development of vasculature in tumors from αCD20/PTX-treated mice (**Fig. 4C**) and our previous results (Andreu et al., 2010).

Given these findings, we examined if the improved PTX response was due to increased numbers of $CD8^+$ T cells, or instead to improved functionality of infiltrating $CD8^+$ T cells by evaluating mRNA expression of SCC infiltrating $CD8^+$ and $CD4^+$ T cells isolated by FACS. Regardless of prior αCD20 treatment, T cells infiltrating SCCs had unchanged

surface expression of activation markers CD69 and CD44 (**Fig. S5D**), and expressed similar levels of $T_H1/T_H2/T_H17$-effectors cytokines (*IL-2, -4, -5, -10, -13, 17a-, 17f, IFNγ, TNFα*) and functional indicators of $CD8^+$ T cell killing capability (e.g., *GzmA, GzmB, Prf1*) (**Fig. S5E**). Although changes to a subset of cells would have been masked by our grouped analysis, these results suggested the improved therapeutic response associated with αCD20/PTX combined therapy was due to reprogramming of the immune microenvironment to favor either survival or infiltration of $CD8^+$ T cells that in turn enhanced tumor cell killing.

Macrophage programming regulates $CD8^+$ T cell recruitment

Given our previous findings that macrophages are functionally reprogrammed to favor a more T_H1-type (classically-activated or 'M1-type') inflammatory state in K14-HPV16 mice lacking either B cells or FcγRs (Andreu et al., 2010), we postulated that αCD20 mAb therapy was similarly reprogramming macrophages in SCCs of treated mice and that a macrophage-dependent mechanism differentially regulated $CD8^+$ T cell infiltration. To investigate this hypothesis, we purified splenic $CD8^+$ T cells (**Fig. S5F**) and evaluated their chemotactic response to conditioned medium derived from FACS-sorted $CD11b^+Ly6C^-Ly6G^-F4/80^+MHCII^+$ macrophages isolated from SCCs of αCD20/PTX versus αRW/PTX-treated mice (**Fig. S5G**), and revealed a significant increase in $CD8^+$ T cell recruitment in response to conditioned medium from αCD20/PTX-derived macrophages (**Fig. 5C**). mRNA expression analysis of $CD11b^+Gr1^-CD11c^-F4/80^+MHCII^+$ macrophages isolated from SCCs of αCD20/PTX-treated versus mice reveled increased mRNA expression of several chemokines variably implicated in leukocyte recruitment including *Ccl2*, *Ccl3*, *Ccl5*, *Ccl7*, and *Ccl9* (**Fig. 5D**), but no significant changes in other genes associated with macrophage repolarization including *Il1b*, *Il6*, Il10, *Il12a*, *Cd163*, *Msr1*, *Arg1, or Ym1* (data not shown). Splenic $CD8^+$ T cells expressed CCR5 (binds CCL3, CCL4 and CCL5) and CXCR3 (binds CXCL10, CXCL11 and CXCL12) (**Fig. S5H**) both of which have been linked to robust anti-tumor responses (Gonzalez-Martin et al., 2011; Hong et al., 2011). Thus, we evaluated the effect of CCR5- and CXCR3-blockade on $CD8^+$ T cell chemotaxis ex vivo and found that an αCCR5-blocking mAb alone abated $CD8^+$ T cell chemotaxis to levels observed with macrophages isolated from SCCs of control αRW/PTX-treated mice (**Fig. 5E**). Importantly, limiting *in vivo* tumor infiltration of macrophages with a neutralizing mAb to colony stimulating factor 1 (αCSF1; **Fig S5I**) blocked the combinatorial effect of αCD20/PTX-treatment (**Fig. 5F**), and restored the density of $CD31^+$ vessels in SCCs to characteristic levels (**Fig. S5J**). The combinatorial effect of αCD20/PTX-treatment was similarly reversed by depletion of $CD8^+$ T cells, and also by use of the CCR5 inhibitor maraviroc (**Fig. 5F**), collectively indicating that response to CTX in SCCs is regulated by CCR5-positive $CD8^+$ T cells responding to macrophages programmed by humoral immunity (**Fig. 6**). In support of a central role for CCL5/CCR5 in mediating a cytotoxic T cell response in SCC patients, we found a significant correlation between expression of *CCL5* and expression of *PRF1*, *GZMA*, *GZMB*, and *CD69* (**Fig. S5K**) in human HNSCC (Ginos et al., 2004).

DISCUSSION

Herein, we provide evidence that therapeutic strategies aimed at depleting B cells and/or dampening humoral immunity represent tractable targets for anti-cancer therapy in SCC. In preclinical prevention and intervention trials, treatment of K14-HPV16 transgenic mice with B cell-depleting αCD20 mAbs or a Syk inhibitor as monotherapy prevented neoplastic progression to the dysplastic/carcinoma in situ state. While SCC growth was significantly slowed in either B cell or FcγR-deficient mice (Andreu et al., 2010), treatment of syngeneic mice bearing preexistent orthotopic SCCs was without consequence following αCD20 mAb monotherapy. However, when αCD20 mAb was delivered in combination with CTX (CDPP, CBDCA and PTX), SCC growth was significantly slowed, accompanied by reduced tumor vascular density and increased T cell infiltration, effects not achieved by administration of CTX alone. Improved SCC response to CTX in αCD20 mAb-treated mice were dependent on presence of “reprogrammed” macrophages producing CCR5 ligands, since depletion of either macrophages or $CD8^+$ T cells restored SCC growth kinetics and vascular density to characteristic levels. Together, these data indicate that myeloid-based pathways regulated by humoral immunity limit SCC responses to CTX not only by fostering tumor angiogenesis, but also by impairing $CD8^+$ T cell infiltration into tumors. Immune microenvironments in solid tumors can therefore be effectively reprogrammed to elicit productive anti-tumor immune responses that bolster response to cytotoxic therapy**,** provided that specific pro-tumoral immune pathways can be identified and therapeutically targeted.

Treatment of solid tumors with CTX, while often useful for palliation or prolonging life in the setting of advanced disease, remains limited with survival benefit often measured in months for some tumor types. Having an adjunctive therapeutic option to reverse or minimize chemo-resistance, or to provide additive benefit through alternate mechanisms (immuno-modulation) represents an attractive therapeutic strategy. Recent approval of ipilimumab, an anti-CTLA4 mAb for use in malignant melanoma (Hodi et al., 2010), and sipileucil-T, a dendritic cell vaccine that prolongs survival but not disease-free survival in hormone-refractory prostate cancer (Kantoff et al., 2010; Small et al., 2006), engenders not only support for immunotherapy in general, but also the concept that immune responses to cancer can be redirected for therapeutic gain. While neither ipilimumab nor sipileucil-T are currently approved for use in conjunction with CTX, it is intriguing to speculate that their efficacy would be improved if administered following CTX, or in combination with therapies that blunt protumor immunity while also favoring an anti-tumor immune microenvironment. Results presented herein reveal that these types of responses can indeed be generated by combining αCD20 mAb with CTX, similarly to that achieved by delivery of CSF1 antagonists with CTX in mammary carcinomas (DeNardo et al., 2011). While both modalities slow tumor growth dependent on $CD8^+$ T cells, these improvements are achieved by distinct molecular mechanisms resulting from lymphoid-based regulation of myeloid cell programming. These distinctions may reflect organ-specific mechanisms governing immune response, or nuances of the oncogenic drivers of solid tumor development.

Clinically, vulva and oropharyngeal malignancies are typically of a high-risk HPV viral etiology (Chaturvedi, 2010), thus K14-HPV16 mice phenocopy neoplastic progression in these tissues and likely recapitulate a protumorigenic role for B cells and/or humoral

immunity in these locales. This assertion is consistent with results from screening a diverse assortment of human solid tumors for evidence of B cell infiltration, i.e., CD20 and/or Ig mRNA expression, wherein vulva and head and neck SCCs contained significantly increased levels of CD20 and Ig mRNA, consistent with histological evaluation of B cells in tumor tissue of these cancers, as well as in human cutaneous SCCs. Several other human tumor types exhibited significant increases in CD20 and/or Ig mRNA as compared to corresponding *normal* tissue. B cell-deficient mice have previously been reported to also resist growth of a range of syngeneic tumors including thymoma, colon, and mammary (Barbera-Guillem et al., 2000; Inoue et al., 2006; Shah et al., 2005; Tadmor et al., 2011), but in most instances these studies utilized non-orthotopic subcutaneous implantation. In several of these models, the pro-tumorigenic role of B cells related to suppression of $CD8^+$ T cell responses either directly through IL-10 (Inoue et al., 2006; Schioppa et al., 2011; Wong et al., 2010) or IL-15 (Chapoval et al., 1998), or indirectly through transforming growth factor (TGF)-β and generation of regulatory T cells (Olkhanud et al., 2011; Tadmor et al., 2011). Whereas our previous findings indicated a role for Igs and CICs in mediating these effects (Andreu et al., 2010; de Visser et al., 2005), in other tumor models, adoptive transfer of B lymphocytes, but not serum, restored tumor growth accompanied by reduced T_H1 cytokines and CTL responses, suggestive of antibody-independent mechanisms (Ammirante et al., 2010; Shah et al., 2005). Since B cells infiltrate human SCCs, unlike what has been observed in murine models of HPV16-induced (Andreu et al., 2010; de Visser et al., 2005) and chemical carcinogenesis-induced (Schioppa et al., 2011) SCCs, we cannot rule out a potential role in human cancers for other B/plasma cell-derived factors such as granulocyte-macrophage (GM)-CSF (Rauch et al., 2012) or lymphotoxin (Moseman et al., 2012), as has been described for growth of subcutaneous androgen-independent metastatic prostate cancer cells (Ammirante et al., 2010).

B cell-depletion as an adjunct to CTX in solid tumors should be relatively straightforward to address clinically. Rituximab is already an approved drug for B cell malignancies (McLaughlin et al., 1998), with no increased susceptibility to infection in patients with adult acute lymphoblastic leukemia, rheumatoid arthritis or non-Hodgkin's lymphoma (Silverman, 2006). This is likely due to the fact that plasma cells are not depleted by αCD20 mAb therapy. We observed “normalized” IgG levels in tumor-bearing mice following αCD20 mAb therapy; thus, targeting pathological production of IgG through depletion of short-lived autoreactive cells without affecting immunity derived from plasma cells could be achieved in solid tumors, similar to that described for arthritis (Huang et al., 2010) and peripheral nervous system autoimmunity (Maurer et al., 2012). Although rituximab has few cumulative side effects and has been combined safely with many CTXs (Gokbuget and Hoelzer, 2006), it should be noted that rituximab has been reported to increase risk of some solid tumors in patients with lymphoma also treated with high-dose CTX and stem cell autografts (Tarella et al., 2011). Alternatively, the clinical success of ibrutinib, an irreversible small molecule inhibitor of BTK (expressed by both B cells and myeloid cell subsets), engenders support for the notion that targeting protumoral B cells and humoral immune-activated pathways may improve overall survival in patients with tumors regulated by these pathways, when administered in combination with standard-of-care CTX.

While studies presented herein identify SCCs as potentially benefiting from αCD20 mAb/CTX, the clinical relevance of αCD20 mAb may not be limited to just these solid tumors. Growth of experimental lung adenocarcinoma is reduced in B cell-deficient mice, with an improved CTX response observed upon co-administration with IL-15, a T_H1 cytokine with IL-2-like anti-tumor bioactivities (Chapoval et al., 1998). Moreover, in a mouse model of melanoma, B cell-deficiency provided a therapeutic advantage to a melanoma vaccine where enhanced tumor protection in the absence of B cells was associated with increased magnitude and longevity of specific cellular immune responses provoked by vaccination (Perricone et al., 2004). We also observed a striking increase in Ig expression in human pancreatic ductal adenocarcinoma samples and are currently evaluating whether this signature translates into a functional role in murine pancreas cancer models. Notably, a limited clinical study of advanced colon cancer patients treated with rituximab resulted in reduced numbers of CD21-hyperpositive lymphocytes associated with apparent 50% reduction in tumor burden with no ill-effects due to therapy (Barbera-Guillem et al., 2000). Since human SCCs appear to be enriched with tumor promoting B cells, we propose these as tractable cancers in which to examine efficacy of αCD20 mAb, or other antagonists blocking protumoral B cell/humoral immunity programs, such as Syk or BTK inhibitors, in combination with CTX.

EXPERIMENTAL PROCEDURES

Microarray data normalization and integration

Microarray data reflecting CD20 and Ig mRNA in human tumor samples were queried from a commercially available dataset (BioExpress® System, Gene Logic Inc., Gaithersburg, MD) originally generated on the Affymetrix Human Genome U133 Plus 2.0 Array (Affymetrix) and normalized by standard Robust Multichip Average (RMA) procedure. A single probe set of the highest variance among samples was chosen to represent CD20 (228592_at; *MS4A1*) and Ig (211430_s_at; *IGHG1*, *IGHG2*, *IGHV4-31*, *IGHM*), respectively. To ensure data consistency, results from additional probe sets were compared to a single probe set. Median value was used to calculate fold change of expression in tumor tissue compared to normal tissue. Statistical analyses were performed using Wilcoxon rank-sum test to compare mRNA expression levels to their corresponding normal tissue controls.

Immunohistochemistry

Staining on human tissue sections was performed as described (Ruffell et al., 2012). De-identified human tissue was received from the UCSF Department of Pathology under approval from the UCSF Committee on Human Research (05028310), and the OHSU Department of Dermatology Molecular Profiling Resource (IRB#809), with patient consent forms obtained at the time of tissue acquisition. The use of samples occurred under “exempt category 4” for individuals receiving de-identified biological specimens.

Animal husbandry and in vivo studies

Generation and characterization of K14-HPV16 and $JH^{-/-}$ mice have been previously described (Andreu et al., 2010). Briefly, K14-HPV16 transgenic mice represent a well-characterized model of multi-stage epithelial carcinogenesis where human papillomavirus

type 16 (HPV16) early region genes are expressed under control of a human keratin 14 (K14) promoter, i.e., K14-HPV16 mice (Arbeit et al., 1994; Coussens et al., 1996; Coussens et al., 1999; Coussens et al., 2000; Daniel et al., 2003; de Visser et al., 2004; de Visser et al., 2005; Rhee et al., 2004; van Kempen et al., 2002). By 1-mo of age, K14-HPV16 mice develop hyperproliferative lesions (hyperplasias) throughout skin. Between 3-6-mo, these progress into 100% penetrant focal dysplasias and are predisposed to progress into multiple histologic grades of SCC in ~50% of mice on the FVB/n strain background, 30% of which metastasize to regional lymph nodes. Angiogenic vasculature is first evident in hyperplasias, development of which is linked to infiltration of innate immune cells (de Visser et al., 2004; de Visser et al., 2005; van Kempen et al., 2002). All experiments with mice complied with National Institutes of Health guidelines and were approved by the UCSF Institutional Animal Care and Use Committee (IACUC).

αCD20 mAB (Clone 5D2; provided by Genentech, Inc.) was generated by immunizing CD20-deficient mice with a murine pre-B cell line (300.19) transfected with murine *CD20*. cDNAs encoding heavy and light chain were cloned from hybridomas and further used for transfection and antibody production in CHO cells. Ragweed specific mouse IgG2a (αRW mAb) was used as an isotype control. K14-HPV16 mice received αCD20 (200 μg) or αRW (200 μg) mAb via i.p. at 2-week intervals commencing at 1 or 3 month of age. Mice bearing syngeneic orthotopic tumors received αCD20 mAb (200 μg) or αRW mAb (200 μg) either at the time of tumor cell inoculation (d0) or following appearance of palpable transplantable tumors (e.g. d12) at 2-week intervals for a total of 3 treatments. K14-HPV16/FcR$\gamma^{+/-}$ (≥18 mice per cohort) and K14-HPV16/FcR$\gamma^{-/-}$ (≥10 mice per cohort) mice were fed chow containing orally soluble fostamatinib (R788) at 2.0 g of fostamatinib per kg of chow, as compared to control chow (AIN-76A) (Rigel Pharmaceuticals) ad libitum beginning at 1 month of age and continuing for a total of 12 weeks. Formulated chow was prepared by Research Diets. R406 (R940406) is the active metabolite of fostamatinib that acts as an ATP-competitive inhibitor (*Ki* =30 nM), thus selectively inhibiting Syk kinase activity as assessed using a large panel of Syk-dependent and -independent cell-based assays (Braselmann et al., 2006). Plasma R406 levels were monitored for 48-, 51-, 54-, 57-, and 58-hrs, revealing peak plasma levels at 558 ng/ml in male FVB/n mice and peak levels in female FVB/n mice at 118.9 ng/ml (data not shown). Thus, using 2.0 mg/ml (10-fold higher than the tested dose), Syk kinase activity in female FVB/n mice was inhibited *in vivo* and was monitored as a function of plasma R406 levels and Syk kinase activity in peripheral blood leukocytes.

Orthotopic tumor transplantation

PDSC5 and WDSC cells (0.5×10^6 cells) were suspended in 100 μl of basement membrane extract Matrigel (BD Pharminogen) in PBS (1:1) and inoculated orthotopically into back skin of 7 week-old female FVB/n mice. Transplantable tumors were measured at 2-day intervals using a digital caliper, and tumor volume calculated using the equation: V (mm^3) = $a \times b^2/2$, (a = largest diameter; b = smallest diameter). To assess effects of paclitaxel (PTX; 12 mg/kg; Novaplus), cisplatin (CDPP; 10 mg/ kg; Hospira), and carboplatin (CBDCA; 50 mg/ kg; APP Pharmaceuticals) on tumor growth, tumor-bearing mice were pretreated with αCD20 mAb or αRW mAb as described above. Chemotherapeutic agents were injected

intravenously at 4-day intervals one week following administration of the second dose of αCD20 or αRW mAb for a total of 3 treatments. Mice were sacrificed 4 days following the last chemotherapeutic dose. For tumor regression studies, mice were treated with αCD20 mAb/PTX following regrowth of transplantable tumors. Mice received PTX at a 4-day interval for a total of 3 treatments. For *in vivo* depletion studies, αCD4 (GK1.5) and αCD8 (YTS169.4) mAb were administered i.p. at 500 μg on day 4 following initial treatment with αCD20 mAb at a 5-day interval, while αCSF1 (5A1) antibodies (all from Bio X Cell) were administered i.p. at 1000 μg 4 days prior to the first chemotherapeutic dose, with subsequent doses of 500 μg every 4 days. Clinical grade maraviroc was dissolved at 300 mg/L in drinking water for ad libitum dosing (Ochoa-Callejero et al., 2013).

Statistical analyses

Statistical analyses were performed using GraphPad Prism version 4 and/or InStat version 3.0a for Macintosh (GraphPad Software). Specific tests included Mann-Whitney (unpaired, nonparametric, two-tailed), unpaired *t*-test, and Wilcoxon rank-sum, and are identified in the respective figures. p values < 0.05 were considered statistically significant with $*p < 0.05$, $**p < 0.01$, $***p < 0.001$ unless otherwise indicated.

Supplementary Material

Refer to Web version on PubMed Central for supplementary material.

Acknowledgments

The authors thank the Knight Cancer Center Flow Cytometry shared resource, Genentech, Inc. for providing αCD20 and αRW mAbs, and members of the Coussens laboratory for critical discussion. The authors also thank the OHSU Department of Dermatology Molecular Profiling Resource (IRB#809) and the OHSU Knight Cancer Institute (NCI P30CA069533) for support of other Shared Core Resources utilized for studies herein. This work was supported by the American Association for Cancer Research and a National Institute of Health postdoctoral training grant in Molecular & Cellular Mechanisms in Cancer (T32 CA108462; N.I.A.), a Department of Defense Breast Cancer Research Program Fellowship (W81XWH-09-1-0543; B.R.), NIH/NCI training grants to TRM (T32CA106195) and AG (T32AI078903-04), and grants from the NIH/NCI (R01 CA130980, R01 CA140943, R01 CA155331, U54 CA163123), a DOD BCRP Era of Hope Scholar Expansion Award (W81XWH-08-PRMRP-IIRA), the Susan B Komen Foundation (KG111084 and KG110560), and the Breast Cancer Research Foundation to LMC.

REFERENCES

Albers A, Abe K, Hunt J, Wang J, Lopez-Albaitero A, Schaefer C, Gooding W, Whiteside TL, Ferrone S, DeLeo A, Ferris RL. Antitumor activity of human papillomavirus type 16 E7-specific T cells against virally infected squamous cell carcinoma of the head and neck. Cancer Res. 2005; 65:11146–11155. [PubMed: 16322265]

Ammirante M, Luo JL, Grivennikov S, Dedospasov S, Karin M. B-cell-derived lymphotoxin promotes castration-resistant prostate cancer. Nature. 2010; 464:302–306. [PubMed: 20220849]

Andreu P, Johansson M, Affara NI, Pucci F, Tan T, Junankar S, Korets L, Lam J, Tawfik D, DeNardo DG, et al. FcRgamma activation regulates inflammation-associated squamous carcinogenesis. Cancer Cell. 2010; 17:121–134. [PubMed: 20138013]

Arbeit JM, Munger K, Howley PM, Hanahan D. Progressive squamous epithelial neoplasia in K14-human papillomavirus type 16 transgenic mice. J Virol. 1994; 68:4358–4368. [PubMed: 7515971]

Arbeit JM, Olson DC, Hanahan D. Upregulation of fibroblast growth factors and their receptors during multi-stage epidermal carcinogenesis in K14-HPV16 transgenic mice. Oncogene. 1996; 13:1847–1857. [PubMed: 8934530]

Bahjat FR, Pine PR, Reitsma A, Cassafer G, Baluom M, Grillo S, Chang B, Zhao FF, Payan DG, Grossbard EB, Daikh DI. An orally bioavailable spleen tyrosine kinase inhibitor delays disease progression and prolongs survival in murine lupus. Arthritis and rheumatism. 2008; 58:1433–1444. [PubMed: 18438845]

Barbera-Guillem E, Nelson MB, Barr B, Nyhus JK, May KF Jr. Feng L, Sampsel JW. B lymphocyte pathology in human colorectal cancer. Experimental and clinical therapeutic effects of partial B cell depletion. Cancer Immunol Immunother. 2000; 48:541–549. [PubMed: 10630306]

Braselmann S, Taylor V, Zhao H, Wang S, Sylvain C, Baluom M, Qu K, Herlaar E, Lau A, Young C, et al. R406, an orally available spleen tyrosine kinase inhibitor blocks fc receptor signaling and reduces immune complex-mediated inflammation. The Journal of pharmacology and experimental therapeutics. 2006; 319:998–1008. [PubMed: 16946104]

Chapoval AI, Fuller JA, Kremlev SG, Kamdar SJ, Evans R. Combination chemotherapy and IL-15 administration induce permanent tumor regression in a mouse lung tumor model: NK and T cell-mediated effects antagonized by B cells. J Immunol. 1998; 161:6977–6984. [PubMed: 9862733]

Chaturvedi AK. Beyond cervical cancer: burden of other HPV-related cancers among men and women. The Journal of adolescent health : official publication of the Society for Adolescent Medicine. 2010; 46:S20–26. [PubMed: 20307840]

Chaturvedi AK, Engels EA, Pfeiffer RM, Hernandez BY, Xiao W, Kim E, Jiang B, Goodman MT, Sibug-Saber M, Cozen W, et al. Human papillomavirus and rising oropharyngeal cancer incidence in the United States. J Clin Oncol. 2011; 29:4294–4301. [PubMed: 21969503]

Colonna L, Catalano G, Chew C, D'Agati V, Thomas JW, Wong FS, Schmitz J, Masuda ES, Reizis B, Tarakhovsky A, Clynes R. Therapeutic targeting of Syk in autoimmune diabetes. J Immunol. 2010; 185:1532–1543. [PubMed: 20601600]

Coussens LM, Hanahan D, Arbeit JM. Genetic predisposition and parameters of malignant progression in K14- HPV16 transgenic mice. Am J Path. 1996; 149:1899–1917. [PubMed: 8952526]

Coussens LM, Raymond WW, Bergers G, Laig-Webster M, Behrendtsen O, Werb Z, Caughey GH, Hanahan D. Inflammatory mast cells up-regulate angiogenesis during squamous epithelial carcinogenesis. Genes Dev. 1999; 13:1382–1397. [PubMed: 10364156]

Coussens LM, Tinkle CL, Hanahan D, Werb Z. MMP-9 supplied by bone marrow-derived cells contributes to skin carcinogenesis. Cell. 2000; 103:481–490. [PubMed: 11081634]

Daniel D, Chiu C, Giraud E, Inoue M, Mizzen LA, Chu NR, Hanahan D. CD4+ T Cell-mediated antigen-specific immunotherapy in a mouse model fo cervical cancer. Cancer Res. 2005; 65:2018–2025. [PubMed: 15753402]

Daniel D, Meyer-Morse N, Bergsland EK, Dehne K, Coussens LM, Hanahan D. Immune enhancement of skin carcinogenesis by CD4+ T cells. J Exp Med. 2003; 197:1017–1028. [PubMed: 12695493]

de Visser KE, Korets LV, Coussens LM. Early neoplastic progression is complement independent. Neoplasia. 2004; 6:768–776. [PubMed: 15720803]

de Visser KE, Korets LV, Coussens LM. De novo carcinogenesis promoted by chronic inflammation is B lymphocyte dependent. Cancer Cell. 2005; 7:411–423. [PubMed: 15894262]

DeNardo DG, Brennan DJ, Rexhepaj E, Ruffell B, Shiao SL, Madden SF, Gallagher WM, Wadhwani N, Keil SD, Junaid SA, et al. Leukocyte Complexity Predicts Breast Cancer Survival and Functionally Regulates Response to Chemotherapy. Cancer Discov. 2011; 1:54–67. [PubMed: 22039576]

Ginos MA, Page GP, Michalowicz BS, Patel KJ, Volker SE, Pambuccian SE, Ondrey FG, Adams GL, Gaffney PM. Identification of a gene expression signature associated with recurrent disease in squamous cell carcinoma of the head and neck. Cancer Res. 2004; 64:55–63. [PubMed: 14729608]

Gokbuget N, Hoelzer D. Novel antibody-based therapy for acute lymphoblastic leukaemia. Best Pract Res Clin Haematol. 2006; 19:701–713. [PubMed: 16997178]

Gonzalez-Martin A, Gomez L, Lustgarten J, Mira E, Manes S. Maximal T cell-mediated antitumor responses rely upon CCR5 expression in both CD4(+) and CD8(+) T cells. Cancer Res. 2011; 71:5455–5466. [PubMed: 21715565]

Gunderson AJ, Coussens LM. B cells and their mediators as targets for therapy in solid tumors. Exp Cell Res. 2013; 319:1644–1649.

Hodi FS, O'Day SJ, McDermott DF, Weber RW, Sosman JA, Haanen JB, Gonzalez R, Robert C, Schadendorf D, Hassel JC, et al. Improved survival with ipilimumab in patients with metastatic melanoma. N Engl J Med. 2010; 363:711–723. [PubMed: 20525992]

Hong M, Puaux AL, Huang C, Loumagne L, Tow C, Mackay C, Kato M, Prevost-Blondel A, Avril MF, Nardin A, Abastado JP. Chemotherapy induces intratumoral expression of chemokines in cutaneous melanoma, favoring T-cell infiltration and tumor control. Cancer Res. 2011; 71:6997–7009. [PubMed: 21948969]

Horikawa M, Minard-Colin V, Matsushita T, Tedder TF. Regulatory B cell production of IL-10 inhibits lymphoma depletion during CD20 immunotherapy in mice. J Clin Invest. 2011; 121:4268–4280. [PubMed: 22019587]

Huang H, Benoist C, Mathis D. Rituximab specifically depletes short-lived autoreactive plasma cells in a mouse model of inflammatory arthritis. Proc Natl Acad Sci U S A. 2010; 107:4658–4663. [PubMed: 20176942]

Inoue S, Leitner WW, Golding B, Scott D. Inhibitory effects of B cells on antitumor immunity. Cancer Res. 2006; 66:7741–7747. [PubMed: 16885377]

Kantoff PW, Higano CS, Shore ND, Berger ER, Small EJ, Penson DF, Redfern CH, Ferrari AC, Dreicer R, Sims RB, et al. Sipuleucel-T immunotherapy for castration-resistant prostate cancer. N Engl J Med. 2010; 363:411–422. [PubMed: 20818862]

Kobayashi A, Darragh T, Herndier B, Anastos K, Minkoff H, Cohen M, Young M, Levine A, Ahdieh Grant L, Hyun W, et al. Lymphoid Follicles Are Generated in High-Grade Cervical Dysplasia and Have Differing Characteristics Depending on HIV Status. Am J Pathol. 2002; 160:151–164. [PubMed: 11786409]

Maurer MA, Rakocevic G, Leung CS, Quast I, Lukacisin M, Goebels N, Munz C, Wardemann H, Dalakas M, Lunemann JD. Rituximab induces sustained reduction of pathogenic B cells in patients with peripheral nervous system autoimmunity. J Clin Invest. 2012; 122:1393–1402. [PubMed: 22426210]

McLaughlin P, White CA, Grillo-Lopez AJ, Maloney DG. Clinical status and optimal use of rituximab for B-cell lymphomas. Oncology (Huntingt). 1998; 12:1763–1769. discussion 1769-1770, 1775-1777. [PubMed: 9874849]

Moseman EA, Iannacone M, Bosurgi L, Tonti E, Chevrier N, Tumanov A, Fu YX, Hacohen N, von Andrian UH. B Cell Maintenance of Subcapsular Sinus Macrophages Protects against a Fatal Viral Infection Independent of Adaptive Immunity. Immunity. 2012; 36:415–426. [PubMed: 22386268]

Nelson BH. CD20+ B cells: the other tumor-infiltrating lymphocytes. J Immunol. 2010; 185:4977–4982. [PubMed: 20962266]

Ochoa-Callejero L, Perez-Martinez L, Rubio-Mediavilla S, Oteo JA, Martinez A, Blanco JR. Maraviroc, a CCR5 antagonist, prevents development of hepatocellular carcinoma in a mouse model. PLoS One. 2013; 8:e53992. [PubMed: 23326556]

Olkhanud PB, Damdinsuren B, Bodogai M, Gress RE, Sen R, Wejksza K, Malchinkhuu E, Wersto RP, Biragyn A. Tumor-evoked regulatory B cells promote breast cancer metastasis by converting resting CD4 T cells to T-regulatory cells. Cancer Res. 2011; 71:3505–3515. [PubMed: 21444674]

Perricone MA, Smith KA, Claussen KA, Plog MS, Hempel DM, Roberts BL, St George JA, Kaplan JM. Enhanced efficacy of melanoma vaccines in the absence of B lymphocytes. J Immunother. 2004; 27:273–281. [PubMed: 15235388]

Qin Z, Richter G, Schuler T, Ibe S, Cao X, Blankenstein T. B cells inhibit induction of T cell-dependent tumor immunity. Nat Med. 1998; 4:627–630. [PubMed: 9585241]

Rauch PJ, Chudnovskiy A, Robbins CS, Weber GF, Etzrodt M, Hilgendorf I, Tiglao E, Figueiredo JL, Iwamoto Y, Theurl I, et al. Innate response activator B cells protect against microbial sepsis. Science. 2012; 335:597–601. [PubMed: 22245738]

Rhee JS, Diaz R, Korets L, Hodgson JG, Coussens LM. TIMP-1 Alters Susceptibility to Carcinogenesis. Cancer Res. 2004; 64:952–961. [PubMed: 14871825]

Rhodes DR, Yu J, Shanker K, Deshpande N, Varambally R, Ghosh D, Barrette T, Pandey A, Chinnaiyan AM. ONCOMINE: a cancer microarray database and integrated data-mining platform. Neoplasia. 2004; 6:1–6. [PubMed: 15068665]

Ruffell B, Au A, Rugo HS, Esserman LJ, Hwang ES, Coussens LM. Leukocyte composition of human breast cancer. Proc Natl Acad Sci U S A. 2012; 109:2796–2801. [PubMed: 21825174]

Schioppa T, Moore R, Thompson RG, Rosser EC, Kulbe H, Nedospasov S, Mauri C, Coussens LM, Balkwill FR. B regulatory cells and the tumor-promoting actions of TNF-alpha during squamous carcinogenesis. Proc Natl Acad Sci U S A. 2011; 108:10661–10667.

Shah S, Divekar AA, Hilchey SP, Cho HM, Newman CL, Shin SU, Nechustan H, Challita-Eid PM, Segal BM, Yi KH, Rosenblatt JD. Increased rejection of primary tumors in mice lacking B cells: inhibition of anti-tumor CTL and TH1 cytokine responses by B cells. Int J Cancer. 2005; 117:574–586. [PubMed: 15912532]

Silverman GJ. Therapeutic B cell depletion and regeneration in rheumatoid arthritis: emerging patterns and paradigms. Arthritis and rheumatism. 2006; 54:2356–2367. [PubMed: 16868991]

Small EJ, Schellhammer PF, Higano CS, Redfern CH, Nemunaitis JJ, Valone FH, Verjee SS, Jones LA, Hershberg RM. Placebo-controlled phase III trial of immunologic therapy with sipuleucel-T (APC8015) in patients with metastatic, asymptomatic hormone refractory prostate cancer. J Clin Oncol. 2006; 24:3089–3094. [PubMed: 16809734]

Tadmor T, Zhang Y, Cho HM, Podack ER, Rosenblatt JD. The absence of B lymphocytes reduces the number and function of T-regulatory cells and enhances the anti-tumor response in a murine tumor model. Cancer Immunol Immunother. 2011; 60:609–619. [PubMed: 21253724]

Tan TT, Coussens LM. Humoral immunity, inflammation and cancer. Curr Opin Immunol. 2007; 19:209–216. [PubMed: 17276050]

Tarella C, Passera R, Magni M, Benedetti F, Rossi A, Gueli A, Patti C, Parvis G, Ciceri F, Gallamini A, et al. Risk factors for the development of secondary malignancy after high-dose chemotherapy and autograft, with or without rituximab: a 20-year retrospective follow-up study in patients with lymphoma. J Clin Oncol. 2011; 29:814–824. [PubMed: 21189387]

van Kempen LCL, Rhee JS, Dehne K, Lee J, Edwards DR, Coussens LM. Epithelial carcinogenesis: dynamic interplay between neoplastic cells and their microenvironment. Differentiation. 2002; 70:501–623.

Wansom D, Light E, Worden F, Prince M, Urba S, Chepeha DB, Cordell K, Eisbruch A, Taylor J, D'Silva N, et al. Correlation of cellular immunity with human papillomavirus 16 status and outcome in patients with advanced oropharyngeal cancer. Archives of otolaryngology--head & neck surgery. 2010; 136:1267–1273. [PubMed: 21173378]

Wong SC, Puaux AL, Chittezhath M, Shalova I, Kajiji TS, Wang X, Abastado JP, Lam KP, Biswas SK. Macrophage polarization to a unique phenotype driven by B cells. Eur J Immunol. 2010; 40:2296–2307. [PubMed: 20468007]

HIGHLIGHTS

- Human SCCs associated with high-risk HPV are infiltrated by Ig-producing B cells
- B cell-depletion or FcγR signaling inhibition impedes SCC neoplastic progression
- Therapeutic B cell-depletion enhances response of established SCCs to chemotherapy
- B cell-depletion reprograms macrophages to recruit $CD8^+$ T cells to SCCs via CCR5

SIGNIFICANCE

The tumor immune microenvironment mediates all aspects of carcinogenesis, targeting of which is an attractive approach for enhancing traditional and targeted anti-cancer therapies. Herein, we identified human SCCs associated with high-risk human papillomaviruses (HPV), as harboring immunoglobulin-producing B cells. Based on this, we evaluated a murine model of HPV16-regulated SCC for efficacy of B cell-depletion as monotherapy, and in combination with standard-of-care chemotherapy. Administration of CD20 monoclonal antibodies significantly improved response to chemotherapy dependent on expression of an altered repertoire of chemokines expressed by macrophages, resulting in increased recruitment of cytotoxic T lymphocytes. These results indicate that the immune microenvironment in susceptible solid tumors can be effectively reprogrammed to foster productive anti-tumor immune responses that bolster response to cytotoxic therapy.

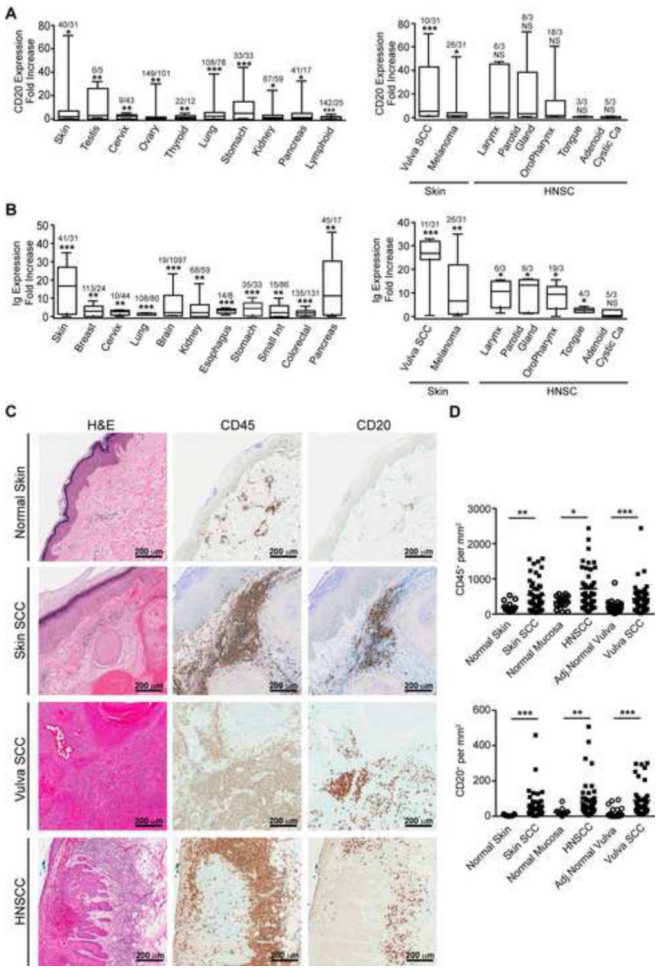

Figure 1. CD20 and Ig mRNA expression in human cancers

Relative CD20 **(A)** and Ig **(B)** mRNA expression in a panel of human cancers. Data are represented as box-and-whisker plots depicting median fold change value compared to normal tissue, displaying the first and third quartiles at the end of each box, with the maximum and minimum at the ends of the whiskers. Number of human cancer tissue / number of normal tissue is shown for each organ. Shown are tissues with statistically significant differences between cancer tissue and control normal tissue, with significance determined via Wilcoxon rank-sum test with *$p < 0.05$, **$p < 0.01$, ***$p < 0.001$. (**C**) Representative histology of skin, vulva, and head and neck SCC in comparison to normal skin tissue. From left to right are (i) H&E, (ii) IHC staining for $CD45^+$ leukocytes, (iii) $CD20^+$ B cells, and $CD8^+$ T cells. (**D**) Density of $CD45^+$, $CD20^+$ and $CD8^+$ cells as determined by automated counting of IHC stained sections. Ca, carcinoma; HNSCC, head and neck squamous carcinoma; SCC, squamous cell carcinoma. See **Fig. S1** for complete analysis.

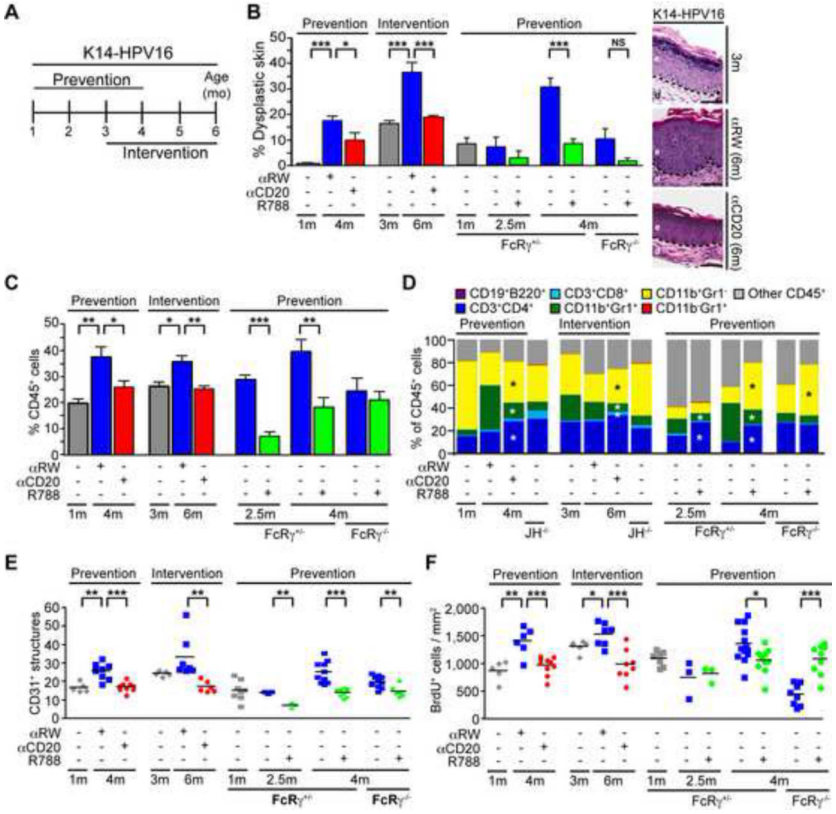

Figure 2. Inhibited neoplastic progression in K14-HPV16 mice by therapeutic αCD20 mAb or fostamatinib

(**A**) Two stages of squamous carcinogenesis were evaluated: (i) K14-HPV16 mice were enrolled at 1 month of age and received αCD20 or isotype control αRW at a 2-week interval until mice were 4 months of age (*Prevention*), and (ii) B cell depletion or Syk inhibition was initiated at 3 months of age at a 2-week interval until mice were 6 months of age (*Intervention*). Fostamatinib (R788), an orally bioavailable Syk kinase inhibitor, was administered through chow ad libitum at 2.0 g/kg/day to HPV16/FcRγ$^{+/-}$ and HPV16/FcRγ$^{-/-}$ mice at 1 month of age as compared to mice receiving control chow until 4 months of age. (**B**) Percentages of ear skin (area) exhibiting dysplasia by 4 or 6 months of age following αCD20 mAb or fostamatinib administration. Values represent percentages of dysplastic lesions compared to whole ear skin per mouse with 5-10 mice per experimental group. Results shown represent mean ± SEM. Representative H&E sections from the αCD20 mAb intervention study are shown to the right. Scale bars are at 50 μm. (**C**) Percentages of CD45$^+$ immune cells in single cell suspensions of skin as assessed by flow cytometry. Results shown represent mean ± SEM. (**D**) Immune cell lineage analysis by flow cytometry as percentages of total CD45$^+$ leukocyte infiltrates in ear tissue. (**E**) Angiogenic vasculature in skin of cohorts as evaluated by CD31/PECAM-1 IHC. Values represent average of five high-power fields of view (FOV) per mouse. (**F**) Keratinocyte proliferation in skin of mice cohorts as assessed by automated counting of bromodeoxyuridine (BrdU)-positive keratinocytes per mm^2 of premalignant tissue. Data reflects ≥ 3 mice per group with statistical significance determined via an unpaired *t*-test with *p < 0.05, **p < 0.01, ***p < 0.001. See also **Fig. S2**.

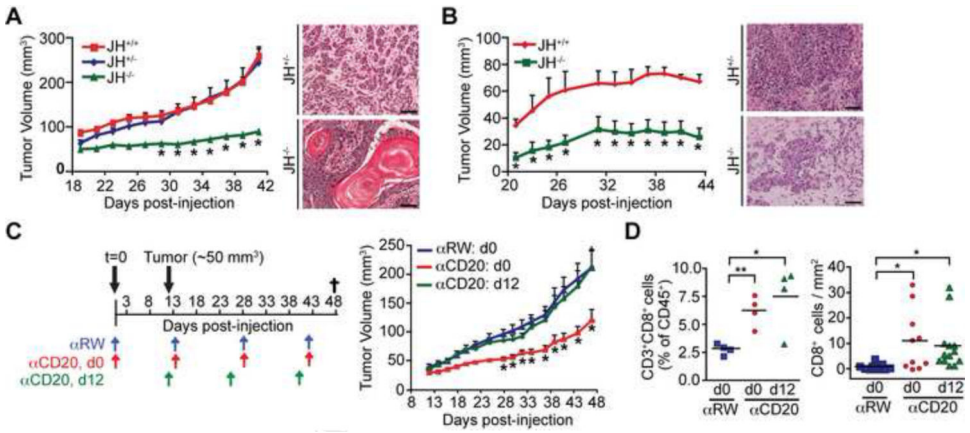

Figure 3. B cell-deficient mice limit SCC tumor growth

Growth of (**A**) PDSC5 (clone 6; PDSC5.6) and (**B**) WDSC1 tumor cells injected orthotopically into syngeneic $JH^{+/+}$ (red), $JH^{+/-}$ (blue), and $JH^{-/-}$ (green) mice. (*) denotes statistically significant differences in tumor growth between $JH^{+/-}$ and $JH^{-/-}$ mice. One of two representative experiments is shown and depicted as mean ± SEM (>10 mice per group). Representative H&E sections are shown to the right. Scale bars are at 50 μm. (**C**) Growth of PDSC5.6-derived tumors in syngeneic mice treated with αCD20 (red) or αRW (blue) mAb either at the time of PDCS5.6 tumor cell inoculation (d0) with 2-week interval dosing (d0, q14d), or alternatively in mice that received αCD20 mAb (green) following appearance of visible tumors (d12, q14d). (*) indicates statistically significant differences between tumor growth in mice receiving αCD20 at d12 compared to αCD20 or αRW at d0. One of two representative experiments is shown depicted as mean ± SEM (≥10 mice per group). (**D**) Infiltration of $CD8^+$ T lymphocytes within tumors from (**C**) as assessed by flow cytometry (left panel) and IHC (right panel). Unless otherwise indicated, statistical significance was determined via an unpaired *t*-test with *$p < 0.05$, **$p < 0.01$. See also **Fig. S3.**

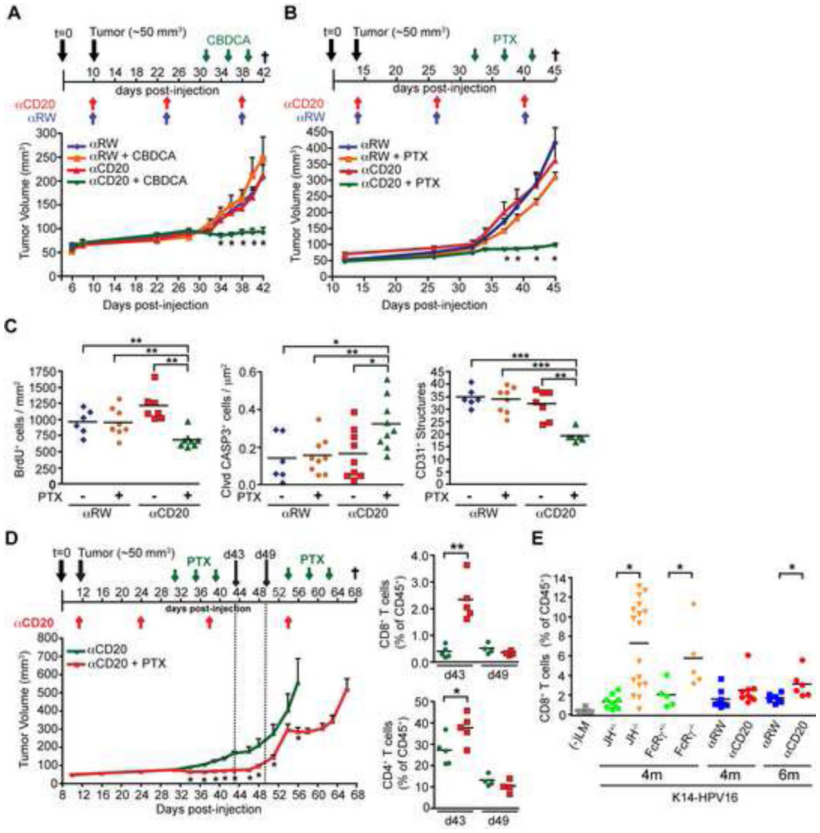

Figure 4. B cell depletion sensitizes established tumors to cytotoxic agents

(**A-B**) Growth of PDSC5.6 SCCs in syngeneic mice receiving αCD20 or αRW mAbs at the time of visible tumor appearance (d10), followed 3 weeks later by administration of the platinum-containing chemotherapeutic agents (**A**) carboplatin (CBDCA; 50 mg/kg; q4dx3) (5-10 mice per group)**,** or (**B**) paclitaxel (PTX; 12 mg/kg; q4dx3), with ≥10 mice per group. One of at least two representative experiments is shown depicted as mean ± SEM with (*) indicating statistically significant differences in tumor growth between αCD20 mAb/CTX, as compared to αCD20 mAb alone. (**C**) Analysis of tissue sections from PDSC5.6 SCCs for (**c**): tumor cell proliferation, apoptosis and vascular density by either automated quantitation of $BrdU^+$, caspase-3^+ cells, or manual counting of $CD31^+$ structures in five high-power fields of view per mouse. (**D**) Growth of PDSC5.6 SCCs in mice receiving multiple cycles of therapy (as shown) (≥17 mice per group). Results shown represent mean ± SEM. Presence of $CD8^+$ and $CD4^+$ T cells in PDSC5.6-derived SCCs, determined by flow cytometry, as percent of total $CD45^+$ leukocytes within tumors at day 43 (stasis) and day 49 (regrowth) shown graphically on right. (**E**) Infiltration of $CD8^+$ T lymphocytes into premalignant skin from 4-mo old K14-HPV16/B cell-deficient, K14-HPV16/FcRγ-deficient, and K14-HPV16 mice enrolled in the Intervention trial with αCD20 mAbs as assessed by flow cytometry as a percentage of $CD45^+$ cells (5-17 mice per group). Unless otherwise indicated, statistical significance was determined via an unpaired *t*-test with *$p < 0.05$, **$p < 0.01$, ***$p < 0.001$. See also **Fig. S4**.

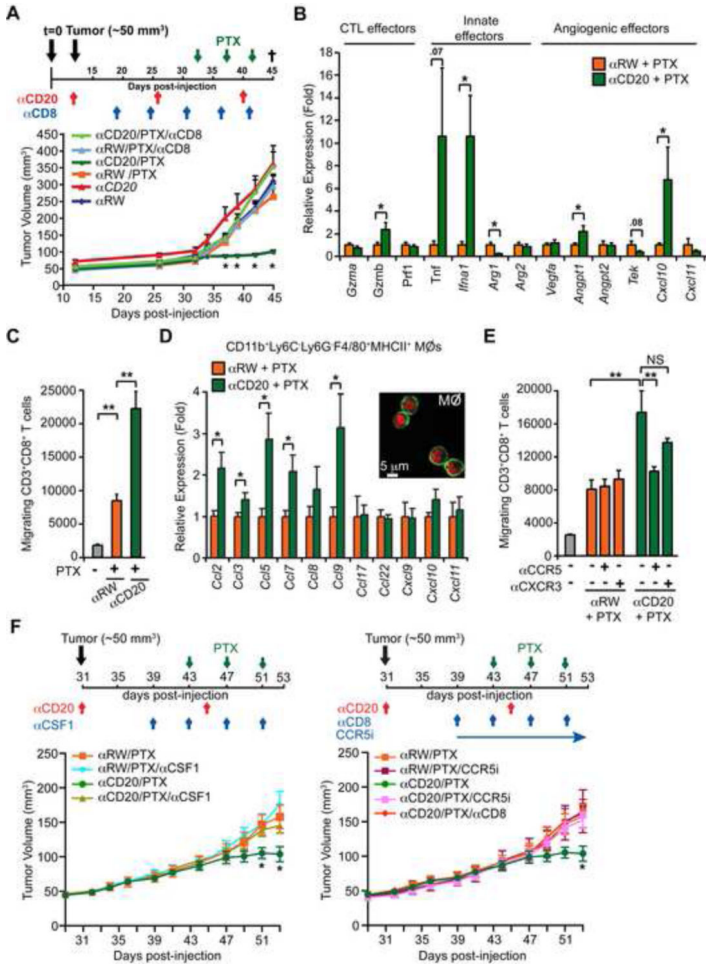

Figure 5. Combination αCD20 mAb plus chemotherapy inhibits SCC tumor growth by CD8$^+$ T cell-dependent mechanisms

(**A**) Tumor growth of PDSC5.6-derived SCCs in mice treated with αCD20 mAb, or αCD8 (clone YTS169.4; 500 μg) depleting mAb, alone or in combination with PTX, as depicted by treatment regimen. One of two representative experiments is shown and depicted as mean ± SEM. (*) indicates statistically significant differences in tumor growth between αCD20/PTX-treated mice compared to mice receiving αCD20 mAb alone (5-10 mice per group). (**B**) mRNA expression of PDSC5.6 SCCs from PBS-perfused αCD20/PTX-treated mice compared to mice receiving αRW/PTX at d45 of treatment regimen. (**C**) Ex vivo recruitment of purified splenic CD8$^+$ T lymphocytes in response to conditioned medium derived from FACS-sorted tumor-associated macrophages (CD11b$^+$Ly6C$^-$Ly6G$^-$F4/80$^+$MHCII$^+$) isolated from PDSC5.6 SCCs of αCD20/PTX versus αRW/PTX-treated mice assessed using a Boyden chamber assay. Data are representative of 2 independent experiments. (**D**) Cytokine mRNA expression of FACS-sorted macrophages (CD11b$^+$Ly6C$^-$Ly6G$^-$F4/80$^+$MHCII$^+$) isolated from PDSC5.6-derived SCCs from αCD20/PTX versus αRW/PTX-treated mice at d45 of treatment regimen. Inset shows representative confocal microscopy showing morphology of sorted macrophages visualized by β-actin (green) and DAPI (red) staining. Data represent mean fold change ± SEM in expression compared to αRW/PTX treatment group (n=8 per group). (**E**) Ex vivo

chemotaxis of purified splenic $CD8^+$ T lymphocytes in response to conditioned medium derived from FACS-sorted macrophages ($CD11b^+Ly6C^-Ly6G^-F4/80^+MHCII^+$) isolated from PDSC5.6 SCCs in αCD20/PTX versus αRW/PTX-treated mice assessed in the presence or absence of blocking antibodies against CCR5 (10 μg/ml) or CXCR3 (10 μg/ml). Samples were assayed in triplicates for each tested condition with pooled samples from 10 tumors. Data are displayed as mean ± SEM. Statistical significance for b-e was determined via an unpaired *t*-test with *p < 0.05, **p < 0.01, ***p < 0.001. (**F**) Relative orthotopic growth of PDSC5.6 SCCs in syngeneic mice following administration of PTX in mice pre-treated with αCD20 mAb, αCD8 depleting mAb (clone YTS169.4), αCSF1 neutralizing mAb (clone 5A1), or the CCR5 inhibitor maraviroc (CCR5i) as depicted by treatment regimen shown. Data represent mean ± 95% SEM. (*) indicates statistically significant differences in tumor growth between αCD20/PTX-treated mice as compared to all other groups as determined by two-way ANOVA (>8 mice per group). See also **Fig. S5.**

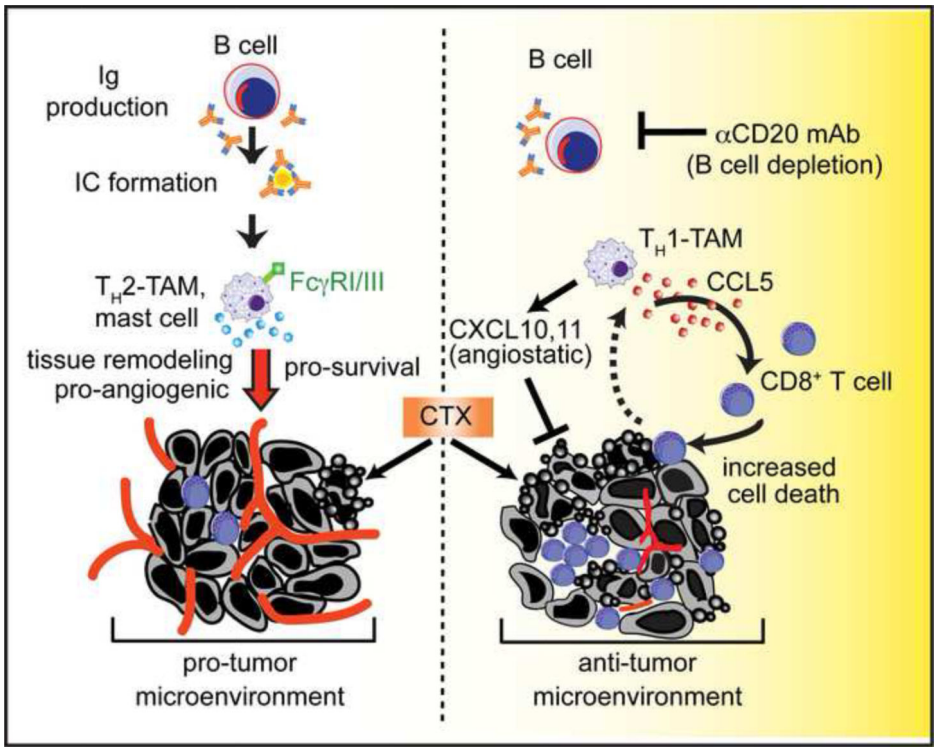

Figure 6. B cell depletion repolarizes tumor-associated macrophages in SCC

Cartoon showing a putative model for improved chemotherapeutic responses in SCCs following B cell depletion. Left: During tumor development, autoantibody production by B cells leads to deposition of immune complexes (IC) within neoplastic tissue. Signaling of these complexes through activating FcγR activates several protumor pathways, including angiogenic, tissue remodeling and pro-survival pathways in mast cells and T_H2-tumor-associated macrophages (TAMs). Right: αCD20 mAb therapy reduces presence of B cells and Ig, the absence of which fosters development of TAMs that instead express increased levels of angiostatic (CXCL10, 11), and CCR chemokines that enhance $CD8^+$ T cell infiltration of malignant tumors culminating in improved response to chemotherapy. Tumor growth to end-stage is thereby significantly slowed by enhanced cytotoxic effects on tumor cells and indirectly through effects on vasculature.